RSC Medicinal Chemistry

ROYAL SOCIETY OF CHEMISTRY

RESEARCH ARTICLE

View Article Online
View Journal

Cite this: DOI: 10.1039/d0md00188k

New imidazo[2,1-*b*]thiazole-based aryl hydrazones: unravelling their synthesis and antiproliferative and apoptosis-inducing potential†

Mohd Adil Shareef,[ab] Ganthala Parimala Devi,[ab] Sunitha Rani Routhu,[c] C. Ganesh Kumar,[c] Ahmed Kamal[bd] and Bathini Nagendra Babu *[ab]

Received 4th June 2020,
Accepted 19th June 2020

DOI: 10.1039/d0md00188k

rsc.li/medchem

Herein, we have designed and synthesized new imidazo[2,1-*b*]thiazole-based aryl hydrazones (**9a–w**) and evaluated their anti-proliferative potential against a panel of human cancer cell lines. Among the synthesized compounds, **9i** and **9m** elicited promising cytotoxicity against the breast cancer cell line MDA-MB-231 with IC_{50} values of 1.65 and 1.12 μM, respectively. Cell cycle analysis revealed that **9i** and **9m** significantly arrest MDA-MB-231 cells in the G0/G1 phase. In addition, detailed biological studies such as annexin V-FITC/propidium iodide, DCFH-DA, JC-1 and DAPI staining assays revealed that **9i** and **9m** triggered apoptosis in MDA-MB-213 cells. Overall, the current work demonstrated the cytotoxicity and apoptosis-inducing potential of **9i** and **9m** in breast cancer cells and suggested that they could be explored as promising antiproliferative leads in the future.

Introduction

Despite meticulous efforts in anticancer drug development, the treatment of malignancy still remains an unsolved challenging health problem. The existing anticancer drugs encounter limitations including drug toxicities due to non-specificity, low efficacy and emergence of multidrug resistance. Therefore, there is a critical need for the development of new chemical entities which can prevail over the aforementioned limitations.[1] Dysregulation of apoptosis is well recognised as a hallmark of cancer.[2] A number of new apoptosis-inducing agents have been identified by researchers. In this context, induction of apoptosis *via* altering the apoptotic pathways has been an emerging approach in the treatment of cancer.[3] Recent reports have revealed that mitochondria are strongly associated with apoptotic pathways and are the major contributor to ROS production.[4] It is evident that excessive levels of ROS enhance basal oxidative stress thereby altering the mitochondrial membrane potential ($\Delta\Psi_m$) and causing mitochondrial dysfunction which eventually triggers apoptosis.[5] The differentiation in ROS levels among normal and cancer cells may possibly offer a prospect of selectively inducing cancer cell demise.[6] So far, a number of ROS-inducing agents with proven anticancer efficacy have been identified.[7,8]

Indeed, the pharmacophore hybridization approach is a rational approach in drug design which enables us to introduce key pharmacophoric subunits into a single moiety. The designed hybrids bearing two scaffolds, if tested, may exhibit synergistic biological activity and reduced side effects.[9] The imidazo[2,1-*b*]thiazole motif has been extensively studied by a vast number of medicinal chemists because of its biologically significant properties including anticancer, anti-hypertensive, antimicrobial, and anti-inflammatory activities.[10] It is reported to be a core nucleus of levamisole (**I**), an anti-helminthic and immunomodulator drug.[11]

Moreover, imidazo[2,1-*b*]thiazoles were found to be effective in postsurgical treatment of Dukes' C colon cancer along with 5-flurouracil (5-FU). Recently, numerous derivatives of imidazo[2,1-*b*]thiazoles (**II–VI**) have been reported as potent anti-proliferative agents exhibiting various molecular mechanisms[12–14] (Fig. 1). Therefore, conjugation of this versatile pharmacophore with other bioactive frameworks might be an exciting tactic in exploration of newer potent chemotherapeutics.

Likewise, the *N*-acylhydrazone (**NAH**) motif is a therapeutically versatile framework for the design and development of newer privileged scaffolds eliciting remarkably extensive biological activities.[15] It can be straightforwardly

[a] *Department of Fluoro-Agrochemicals, CSIR-Indian Institute of Chemical Technology, Tarnaka, Hyderabad, India. E-mail: bathini@iict.res.in*
[b] *Academy of Scientific and Innovative Research, Ghaziabad 201 002, India*
[c] *Organic Synthesis and Process Chemistry Division, CSIR-Indian Institute of Chemical Technology, Tarnaka, Hyderabad 500007, India*
[d] *School of Pharmaceutical Education and Research (SPER), Jamia Hamdard, New Delhi 110062, India*

† Electronic supplementary information (ESI) available. See DOI: 10.1039/d0md00188k

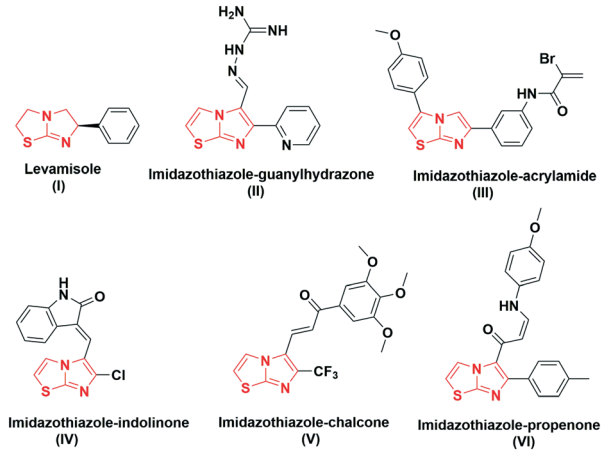

Fig. 1 Structure of levamisole and some imidazo[2,1-*b*]thiazole derivatives exhibiting anti-proliferative activity.

synthesised *via* a condensation reaction. Moreover, various drugs such as azumolene, carbazochrome, dantrolene, nitrofurantoin, nifuroxazide, *etc.* endowed with the *N*-acylhydrazone (**NAH**) backbone are presently used in the clinic. In addition, a number of potential anticancer leads such as LASSBio-1586 (**VII**), PAC-1 (**VIII**) and aldoxorubicin (Fig. 2) are now in pre-clinical and/or clinical trials.[16] Consequently, these facts suggested that the *N*-acylhydrazone (**NAH**) motif could be incorporated for the search of newer cytotoxic agents in the current research context.[17]

Encouraged by the bioactivities of imidazo[2,1-*b*]thiazoles and *N*-acylhydrazones, and in progression with our exploitation towards the development of newer apoptosis inducers,[18] we herein synthesized imidazo[2,1-*b*]thiazole-based aryl hydrazones by hybridizing the imidazo[2,1-*b*]thiazole motif and *N*-acylhydrazone moiety (Fig. 3). The synthesized compounds were tested for their antiproliferative activity. The promising activity observed encouraged us to investigate the effect of these compounds on apoptosis.

Chemistry

Imidazo[2,1-*b*]thiazole-based aryl hydrazones (**9a–w**) were synthesized as shown in Scheme 1. At first, substituted

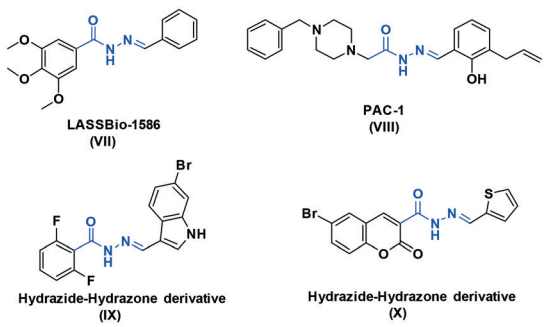

Fig. 2 Structures of some *N*-acyl hydrazone (**NAH**) derivatives exhibiting anti-proliferative activity.

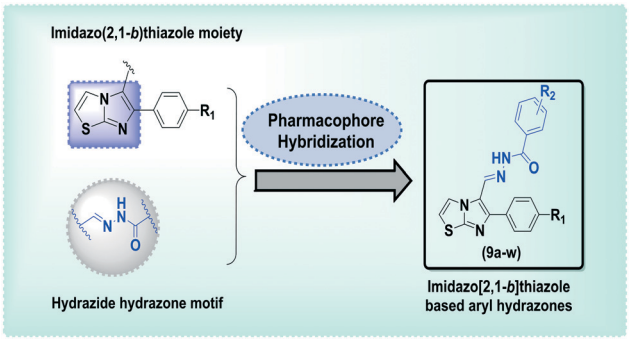

Fig. 3 Design strategy of new imidazo[2,1-*b*]thiazole-based aryl hydrazones (**9a–w**).

2-bromoacetophenones (**1a–d**) and 2-aminothiazole (**2**) in equimolar quantities were refluxed in acetone for 6–8 h followed by addition of 2N HCl. The reaction was again refluxed for 1–2 h to yield imidazo[2,1-*b*]thiazoles (**4a–d**). These intermediates were later subjected to Vilsmeier–Haack reaction conditions to obtain the corresponding imidazo[2,1-*b*]thiazole carboxaldehydes (**5a–d**).[19] Similarly, substituted benzoic acids were subjected to esterification to obtain the corresponding esters which upon further treatment with hydrazine hydrate in ethanol under reflux conditions

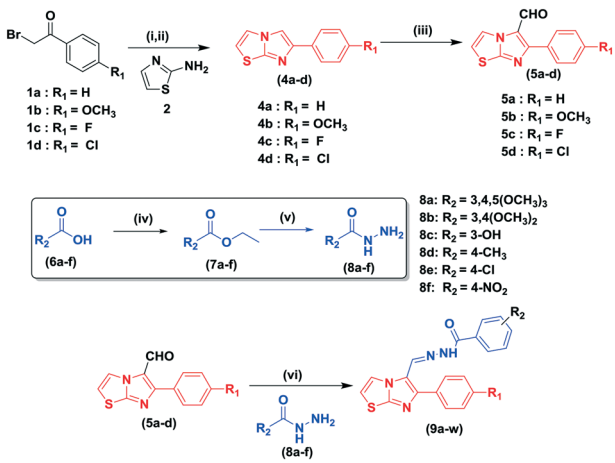

	R_1	R_2		R_1	R_2
9a	H	3,4,5-trimethoxyphenyl	**9m**	4-F	3,4,5-trimethoxyphenyl
9b	H	3,4-dimethoxyphenyl	**9n**	4-F	3,4-dimethoxyphenyl
9c	H	3-hydroxyphenyl	**9o**	4-F	3-hydroxyphenyl
9d	H	4-methylphenyl	**9p**	4-F	4-methylphenyl
9e	H	4-chlorophenyl	**9q**	4-F	4-chlorophenyl
9f	H	4-nitrophenyl	**9r**	4-F	4-nitrophenyl
9g	4-OCH_3	3,4,5-trimethoxyphenyl	**9s**	4-Cl	3,4,5-trimethoxyphenyl
9h	4-OCH_3	3,4-dimethoxyphenyl	**9t**	4-Cl	3,4-dimethoxyphenyl
9i	4-OCH_3	3-hydroxyphenyl	**9u**	4-Cl	3-hydroxyphenyl
9j	4-OCH_3	4-methylphenyl	**9v**	4-Cl	4-methylphenyl
9k	4-OCH_3	4-chlorophenyl	**9w**	4-Cl	4-chlorophenyl
9l	4-OCH_3	4-nitrophenyl			

Scheme 1 Synthesis of new imidazo[2,1-*b*]thiazole-based aryl hydrazones (**9a–w**). Reagents and conditions: (i) acetone, reflux, 6–8 h; (ii) 2N HCl, reflux, 1–2 h, 85–90%; (iii) $POCl_3$, DMF, reflux, 8–12 h, 80–88%; (iv) H_2SO_4, EtOH, reflux, 2–3 h, 90–95%; (v) $NH_2NH_2{\cdot}5H_2O$, EtOH, reflux, 6–8 h, 82–89%; (vi) EtOH, few drops of glacial acetic acid, reflux, 3–6 h, 72–85%.

provided the aryl hydrazide precursors (**8a–f**).[20] Lastly, the corresponding imidazo[2,1-*b*]thiazole carboxaldehydes (**5a–d**) were condensed with appropriate aryl hydrazide precursors (**8a–f**) in absolute ethanol in the presence of a catalytic amount of glacial acetic acid for 3–6 h to attain the final compounds (**9a–w**) in good yields. The structure of all the titled compounds was established by suitable spectroscopic techniques.

Biological evaluation

Anti-proliferative activity. The synthesized imidazo[2,1-*b*]thiazole-based aryl hydrazones (**9a–w**) were tested for their antiproliferative activity in selected human cell lines of prostate cancer (DU-145), breast cancer (MDA-MB-231), cervical cancer (HeLa), lung cancer (A549) and normal embryonic kidney cancer cells (HEK-293) by using the MTT assay.[21] The IC_{50} values (μM) are presented in Table 1.

The cell lines MDA-MB-231 (ATCC No. HTB-26), HEK-293 (ATCC No. CRL-1268), DU-145 (ATCC No. HTB-81), HeLa (ATCC No. CCL-2) and A549 (ATCC No. CCL-185) were purchased from ATCC. The synthesized compounds were tested on other cancer cell lines [prostate cancer (DU-145), cervical cancer (HeLa) and lung cancer (A549)] and were found to be unresponsive at levels below 5 micromolar concentration. Among the tested derivatives, compounds **9a**, **9i** and **9m** exhibited significant cytotoxicity with IC_{50} values ranging between 1.12 and 5.2 μM against the tested cell lines. Interestingly, compounds **9i** and **9m** exhibited promising cytotoxicity against the breast cancer line (MDA MB-231) with IC_{50} values of 1.65 and 1.12 μM, respectively. From a structure–activity relationship perspective, it was observed that compound **9m** was the most potent wherein $\mathbf{R_1}$ was substituted with electronegative substituent 4-F and $\mathbf{R_2}$ was substituted with an electron donating 3,4,5-trimethoxy group; while in the case of compound **9i**, both $\mathbf{R_1}$ and $\mathbf{R_2}$ were substituted by electron donating groups such as 4-methoxy and 3,4,5-trimethoxy, respectively, which exhibited promising cytotoxicity as compared to other screened molecules in the series. Furthermore, in the case of compound **9a**, which was one of the potential compounds, $\mathbf{R_1}$ was unfunctionalized and $\mathbf{R_2}$ was substituted with an electron donating 3,4,5-trimethoxy group. Overall, electron donating substituents such as 3,4,5-trimethoxy and hydroxyl were found to be favourable for cytotoxicity at $\mathbf{R_2}$, while there was no noteworthy alteration in the cytotoxicity by switching from electron donating groups to electron donating groups at $\mathbf{R_1}$.

Table 1 Antiproliferative activity of the synthesized imidazo[2,1-*b*]thiazole-based aryl hydrazones (**9a–w**)

IC_{50} values in[a] μM of the synthesized compounds		
CODE	MDA-MB-231[b]	HEK-293[c]
9a	3.1 ± 0.82	24.6 ± 1.2
9b	12.3 ± 0.52	—[d]
9c	18.6 ± 0.22	—
9d	>50	—
9e	12.9 ± 0.39	—
9f	21.0 ± 0.32	—
9g	15.3 ± 0.44	—
9h	21.4 ± 0.29	—
9i	**1.65 ± 0.37**	39.9 ± 1.1
9j	17.2 ± 0.18	—
9k	20.8 ± 0.29	—
9l	25.5 ± 0.32	—
9m	**1.12 ± 0.43**	48.1 ± 0.53
9n	11.8 ± 0.32	—
9o	18.0 ± 0.39	—
9p	14.0 ± 0.35	—
9q	35.5 ± 0.38	—
9r	15.3 ± 0.24	—
9s	19.8 ± 0.23	—
9t	>50	—
9u	14.6 ± 0.17	—
9v	24.2 ± 0.24	—
9w	15.7 ± 0.49	—
Doxorubicin	0.8 ± 0.09	—

[a] Concentration required to inhibit 50% of cell growth and the values represent the mean of three independent experiments. [b] Breast cancer. [c] Normal human embryonic kidney cells. [d] Not determined; bold values signify promising activity.

Cell cycle analysis

The potential compounds **9i** and **9m** were further studied for growth inhibition of cancer cells by arresting the cell cycle checkpoint that facilitates the development of potent cytotoxic agents.[22] MDA-MB-231 cells were treated with 1 μM of test compounds **9i** and **9m** for 24 h wherein doxorubicin was used as a positive control.[23] Flow cytometry revealed that test compounds **9i** and **9m** caused the G0/G1 cell cycle arrest with 72.4% and 75.8% cells accumulated (Fig. 4) when compared to untreated cells (control). The positive control, doxorubicin treatment, caused accumulation of 81% of cells in the G0/G1 phase (Fig. 4). In Fig. 4, M4 represents the G0/G1 phase while M5 and M6 represent the S phase and G2/M phase, respectively. Cell cycle analysis suggested that there is a significant increase in the arrest of cells in the G0/G1 phase when compared to the control.

Quantification of apoptosis by the annexin V-FITC/propidium iodide staining assay

In order to determine the apoptotic induced cell death, annexin V FITC and propidium iodide staining was performed by using an annexin V-FITC apoptosis detection kit.[24] The results were interpreted as the percentage of total cells appearing in each quadrant. This assay facilitates the detection of live cells (Q1-LL; AV−/PI−), early apoptotic cells (Q1-LR; AV+/PI−), late apoptotic cells (Q1-UR; AV+/PI+) and necrotic cells (Q1-UL; AV−/PI+). In this study, MDA-MB-231 cells were treated with the tested compounds for 24 h at 1 and 2 μM concentrations, respectively. The distribution of apoptotic and necrotic cells upon treatment with various concentrations of **9i** and **9m** is shown in Fig. 5. The results to this regard are presented in Table 2. The results indicated

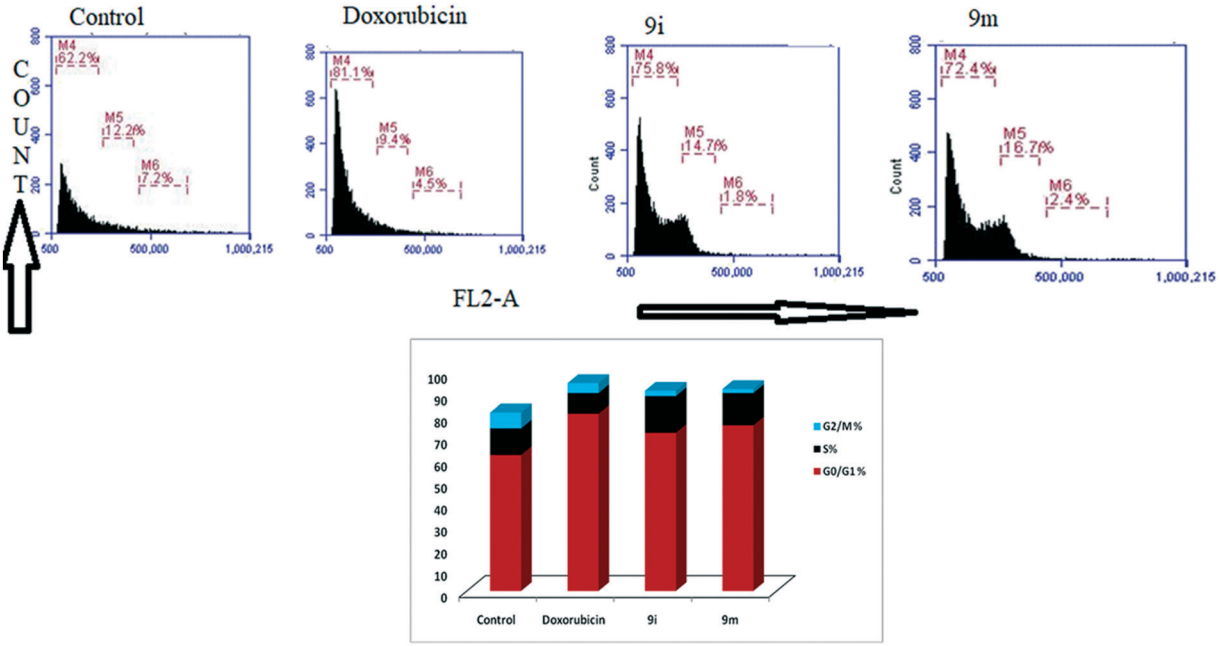

Fig. 4 Flow cytometric analysis in the MDA-MB-231 breast cancer cell line after treatment with compounds **9i** and **9m** at 1 μm concentration for 24 h. Graphical representation of cell cycle analysis. M4 represents the G0/G1 phase; M5 and M6 represent the S phase and G2/M phase, respectively.

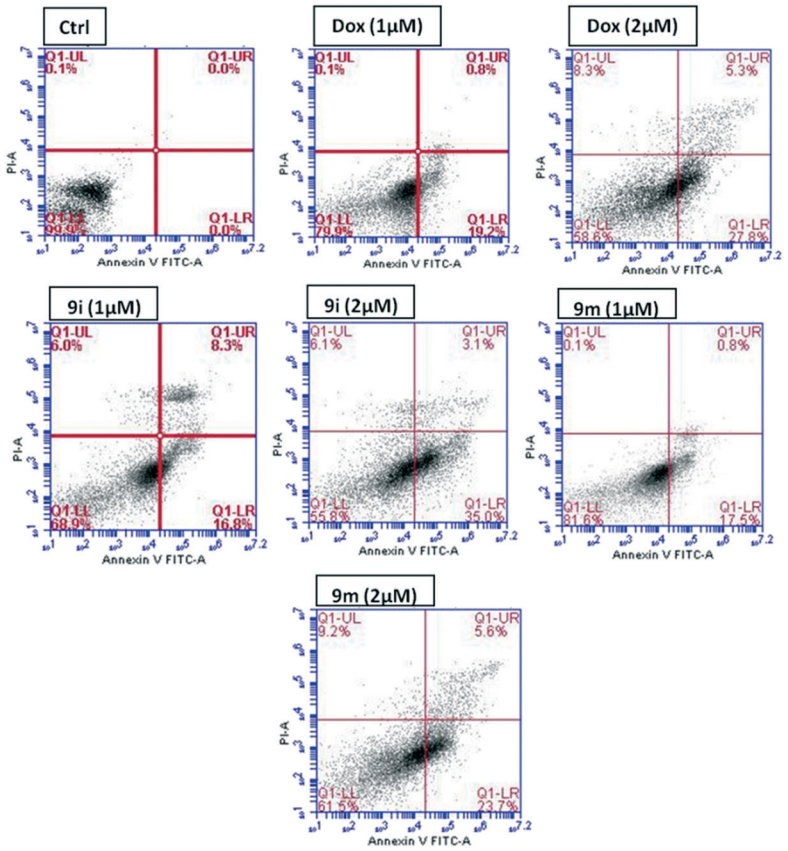

Fig. 5 Annexin V-FITC/propidium iodide dual staining assay.

Table 2 Distribution of apoptotic cells based on annexin-V FITC experiments

	Lower left	Lower right	Upper right	Upper left
Sample (concentration)	Live cells (%)	Early apoptosis (%)	Late apoptosis (%)	Necrosis (%)
MDA-MB-231 (untreated)	99.9 ± 0.02	0.0	0.0	0.1 ± 0.04
Doxorubicin (1 μM)	79.9 ± 0.012	19.2 ± 0.23	0.8 ± 0.01	0.1 ± 0.023
Doxorubicin (2 μM)	58.6 ± 0.013	27.8 ± 0.11	5.3 ± 0.01	8.3 ± 0.024
9i (1 μM)	67.6 ± 0.08	16.8 ± 0.27	8.3 ± 0.03	6.0 ± 0.025
9i (2 μM)	55.8 ± 0.34	35.0 ± 0.21	3.1 ± 0.04	6.1 ± 0.021
9m (1 μM)	81.6 ± 0.23	17.5 ± 0.01	0.8 ± 0.06	0.1 ± 0.06
9m (2 μM)	61.5 ± 0.12	23.7 ± 0.23	5.6 d± 0.03	9.2 ± 0.056

Note: the experiment was performed in triplicate and the results are represented as mean ± standard deviation.

that the percentage of early apoptotic cells in compound-treated wells considerably increased when compared with the control and standard drug. The results revealed that these compounds induced cell death *via* early apoptosis in a concentration-dependent manner in human breast cancer cells.

DAPI staining

DAPI (4′,6-diamidino-2-phenylindole) is a nuclear stain that can envisage nuclear morphological changes which are characteristic features of apoptosis. DAPI stains the apoptotic cells in bright colour because of the condensed nucleus which is a characteristic feature of apoptosis.[25] Therefore, DAPI staining of compounds **9i** and **9m** (1 μM) in the breast cancer cell line (MDA-MB-231) was carried out to study the morphological changes induced by doxorubicin (1 μM) which was used as the standard, and the cells were treated for 48 h. The control cells displayed large sized intact nuclei, while **9i** and **9m** treated cells displayed fragmented, abnormally shaped nuclei characteristic of apoptosis. In addition, higher numbers of condensed apoptotic cells were observed in **9i** and **9m** treated samples (Fig. 6).

Quantitative estimation of ROS generation by DCFH-DA staining

Increased levels of intracellular reactive oxygen species (ROS) may cause oxidative damage leading to loss of mitochondrial membrane potential which further leads to initiation of the intrinsic pathway of apoptosis and eventual cell death.[26] Hence efforts were made to determine the effect of compounds **9i** and **9m** on the intracellular ROS generation through a peroxide sensitive fluorescent dye, 2′-7′-dichlorodihydro-fluorescein diacetate (DCFH-DA), staining method in MDA-MB-231 cells.[27] DCFH-DA is a non-fluorescent cell permeable dye which upon entering the cells becomes oxidized by esterases in the cytosol and converts into non-diffusible green fluorescent DCF. Treatment with compounds **9i** and **9m** for 6 h resulted in a considerable rise in DCFH-DA fluorescence when compared to control cells, demonstrating the ROS accumulating potential of the compounds which signifies that the compounds promote apoptosis (Fig. 7).

Analysis of mitochondrial membrane potential by JC-1 staining

The alteration of the mitochondrial electrochemical potential (MMP) gradient ($\Delta\Psi_m$) is known as an early event in drug-

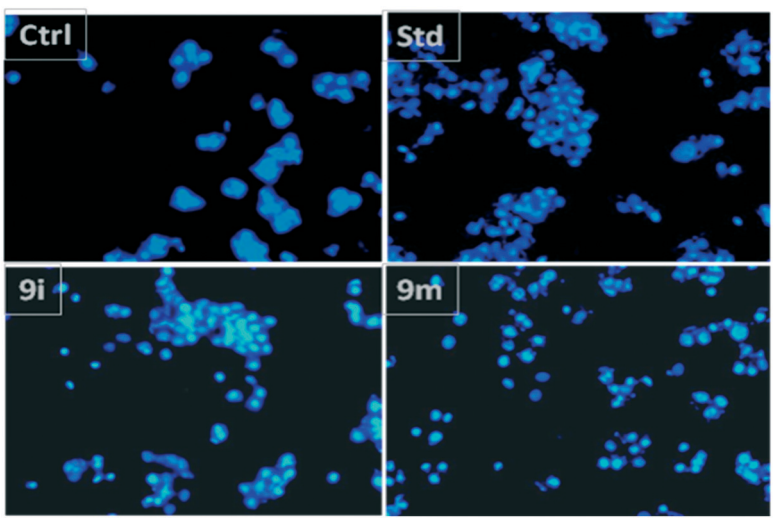

Fig. 6 Effect of compounds **9i** and **9m** on the nuclear morphology of MDA-MB-231 cells stained with DAPI. The images were captured using a fluorescence microscope at 100× magnification.

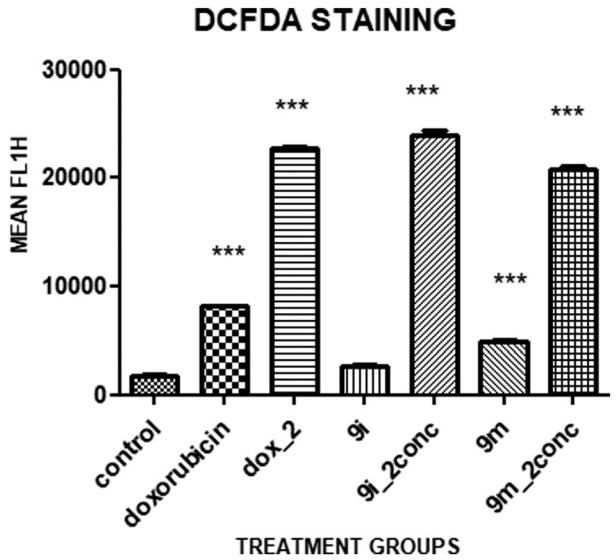

Fig. 7 Effect of compounds **9i** and **9m** on intracellular reactive oxygen species (ROS) levels. Mean FL1H represents fluorescence units in the green filter.

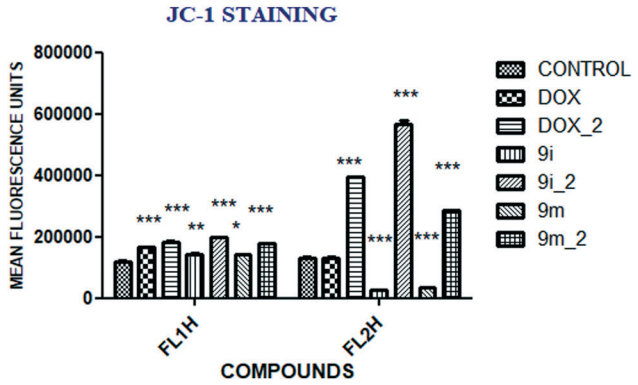

Fig. 8 Effect of compounds **9i** and **9m** on mitochondrial potential ($\Delta\Psi_m$).

induced apoptosis. According to previous reports, mitochondrial membrane injury, loss of mitochondrial membrane potential and induction of intracellular ROS levels are directly connected events which trigger apoptosis.[28] Hence, we herein assessed the ability of compounds **9i** and **9m** to promote apoptosis in cancerous cells by the mitochondrial regulated mechanism, by evaluating the changes in the MMP ($\Delta\Psi_m$) of MDA-MB-213 cells using cationic JC-1 staining using a flow cytometer. The uptake of the dye by the mitochondria showed effective distinction between apoptotic cells and healthy cells. After 24 h of drug treatment with the tested compounds at 1 μM and 2 μM concentrations, the results presented in Fig. 8 revealed that there was a reduction in the mitochondrial membrane potential ($\Delta\Psi_m$) of MDAMB-213 cells in a dose-dependent manner when compared to doxorubicin.

MDA-MB 231 cells were treated with the test compounds and the samples were then analyzed using flow cytometry on an FAC Scan (Becton Dickinson) in the FL1 and FL2 channels to detect the mitochondrial potential. In the *X*-axis, FL1H represents mean fluorescence units in the green filter. FL2H represents mean fluorescence units in the red filter. The *Y*-axis represents mean fluorescence units.

Conclusion

In the present study, we have synthesized a series of imidazo[2,1-*b*]thiazole-based aryl hydrazones (**9a–w**) and evaluated them for their anti-proliferative activity. Among them, **9a**, **9i** and **9m** exhibited significant cytotoxicity with IC_{50} values ranging between 1.12 and 5.2 μM against the tested cell lines. Interestingly, compounds **9i** and **9m** exhibited promising cytotoxicity against the breast cancer cell line MDA-MB-231 with IC_{50} values of 1.65 and 1.12 μM, respectively. Further, **9i** and **9m** exhibited a significant increase in the arrest of cells in the G0/G1 phase of the cell cycle when compared to the control. Detailed biological studies, including the annexin V-FITC assay, DAPI staining, DCFH-DA assay and JC-1 staining, suggested that these potential compounds induce apoptosis in the breast cancer cell line. Based on these results, compounds **9i** and **9m** were found to be effective cytotoxic agents and could be further developed as prime anti-proliferative agents.

Conflicts of interest

The authors declare no conflict of interest.

Acknowledgements

The authors would like to thank CSIR, UGC and UGC-MANF, New Delhi for the funding and the Director, CSIR-IICT for the support (Manuscript Communication number: IICT/Pubs./2019/396).

References

1 (*a*) R. L. Siegel, K. D. Miller and A. Jemal, *Ca-Cancer J. Clin.*, 2019, **69**, 7–34; (*b*) R. W. Robey, K. M. Pluchino, M. D. Hall, A. T. Fojo, S. E. Bates and M. M. Gottesman, *Nat. Rev. Cancer*, 2018, **18**, 452–464.

2 W. M. Eldehna, G. S. Hassan, S. T. Al-Rashood, T. Al-Warhi, A. E. Altyar, H. M. Alkahtani, A. A. Almehizia and H. A. Abdel-Aziz, *J. Enzyme Inhib. Med. Chem.*, 2019, **34**, 322–332.

3 (*a*) A. M. S. El-Sharief, Y. A. Ammar, A. Belal, M. A. M. S. El-Sharief, Y. A. Mohamed, A. B. M. Mehany, G. A. M. Elhag Ali and A. Ragab, *Bioorg. Chem.*, 2019, **85**, 399–412; (*b*) R. C. Taylor, S. P. Cullen and S. J. Martin, *Nat. Rev. Mol. Cell Biol.*, 2008, **9**, 231–241.

4 (*a*) L. Jina, L. Daib, M. Jia and H. Wang, *Bioorg. Chem.*, 2019, **85**, 179–190; (*b*) J. Lopez and S. W. G. Tait, *Br. J. Cancer*, 2015, **112**, 957–962.

5 (*a*) M. Redza-Dutordoir and D. A. Averill-Bates, *Biochim. Biophys. Acta*, 2016, **1863**, 2977–2992; (*b*) Y. Wang, C. Wu, Q.

Zhang, Y. Shan, W. Gu and S. Wang, *Bioorg. Chem.*, 2019, **84**, 468–477.

6 X.-J. Shi, B. Yu, J.-W. Wang, P.-P. Qi, K. Tang, X. Huang and H.-M. Liu, *Sci. Rep.*, 2016, **6**, 31607–31619.

7 W. Liang, J. Cui, K. Zhang, H. Xi, A. Cai, J. Li, Y. Gao, C. Hu, Y. Liu, Y. Lu, N. Wang, X. Wu, B. Wei and L. Chen, *Oncotarget*, 2017, **8**, 109094–109106.

8 T. Ma, Q. S. Ma, B. Yu and H. M. Liu, *Eur. J. Med. Chem.*, 2019, **174**, 76–86.

9 C. V. Junior, A. Danuello, V. da Silva Bolzani, E. J. Barreiro and C. A. Fraga, *Curr. Med. Chem.*, 2007, **14**, 1829–1852.

10 M. A. Shareef, I. Khan, B. N. Babu and A. Kamal, *Curr. Med. Chem.*, 2019, **26**, 1–24.

11 (*a*) R. I. Fenichel, M. A. Chirigos and C. H. Hoerig, *Immune modulation agents and their mechanism*, Marcel Dekker Inc., NY, Basel, 1984, pp. 383–408; (*b*) S. Koppireddi, D. R. Chilaka, S. Avula, J. R. Komsani, S. Kotamraju and R. Yadla, *Bioorg. Med. Chem. Lett.*, 2014, **24**, 5428–5431; (*c*) A. Kamal, G. B. R. Khanna, T. Krishnaji and R. Ramu, *Bioorg. Med. Chem. Lett.*, 2005, **15**, 613–615.

12 (*a*) R. Romagnoli, P. G. Baraldi, F. Prencipe, J. Balzarini, S. Liekens and F. Estévez, *Eur. J. Med. Chem.*, 2015, **101**, 205–217; (*b*) I. B. Sayeed, K. R. Garikapati, V. K. K. Makani, A. Nagarajan, M. A. Shareef, A. Alarifi, M. Pal-Bhadra and A. Kamal, *ChemistrySelect*, 2017, **2**, 6480–6487.

13 A. Andreani, M. Granaiola, A. Leoni, A. Locatelli, R. Morigi, M. Rambaldi, V. Garaliene, W. Welsh, S. Arora, G. Farruggia and L. O. Masotti, *J. Med. Chem.*, 2005, **48**, 5604–5607.

14 M. F. Baig, V. L. Nayak, B. Prasad, M. Kishore, S. Sunkari, J. Gour and A. Kamal, *Bioorg. Chem.*, 2018, **77**, 515–526.

15 S. Thota, D. A. Rodrigues, P. de Sena, M. Pinheiro, L. M. Lima, C. A. M. Fraga and E. J. Barreiro, *Bioorg. Med. Chem. Lett.*, 2018, **28**, 2797–2806.

16 (*a*) A. D. Joshi, R. C. Botham, L. J. Schlein, H. S. Roth, A. Mangraviti, A. Borodovsky, B. Tyler, S. Joslyn, J. S. Looper, M. Podell, T. M. Fan, P. J. Hergenrother and G. J. Riggins, *Oncotarget.*, 2017, **8**, 80124–80138; (*b*) E. Sachdev, D. Sachdev and M. Mita, *Expert Opin. Invest. Drugs*, 2017, **26**, 1175–1179.

17 (*a*) T. Nasr, S. Bondock and M. Youns, *Eur. J. Med. Chem.*, 2014, **76**, 539–548; (*b*) B. Aneja, N. S. Khan, P. Khan, A. Queen, A. Hussain, M. T. Rehman, M. F. Alajmi, H. R. El-Seedi, S. Ali, M. I. Hassan and M. Abid, *Eur. J. Med. Chem.*, 2019, **163**, 840–852; (*c*) H. He, X. Wang, L. Shi, W. Yin, Z. Yang, H. He and Y. Liang, *Bioorg. Med. Chem. Lett.*, 2016, **26**, 3263–3270.

18 (*a*) S. Sunkari, S. R. Bonam, A. V. S. Rao, S. Riyaz, V. L. Nayak, H. M. S. Kumar, A. Kamal and B. N. Babu, *Bioorg. Chem.*, 2019, **87**, 484–494; (*b*) A. Nagarsenkar, L. Guntuku, S. D. Guggilapu, K. D. Bai, S. Gannoju, V. G. M. Naidu and B. N. Babu, *Eur. J. Med. Chem.*, 2016, **124**, 782–793.

19 M. A. Shareef, K. Sirisha, I. B. Sayeed, I. Khan, T. Ganapathi, S. Akbar, G. Kumar, A. Kamal and B. N. Babu, *Bioorg. Med. Chem. Lett.*, 2019, **19**, 126621–126626.

20 A. Kamal, P. S. Srikanth, M. V. Vishnuvardhan, G. B. Kumar, K. S. Babu, S. M. A. Hussaini, J. S. Kapure and A. Alarifi, *Bioorg. Chem.*, 2016, **65**, 126–136.

21 M. Botta, S. Armaroli, D. Castagnolo, G. Fontana, P. Perad and E. Bombardelli, *Bioorg. Med. Chem. Lett.*, 2007, **17**, 1579–1583.

22 (*a*) K. T. Chan, F. Y. Meng, Q. Li, C. Y. Ho, T. S. Lam, Y. To, W. H. Lee, M. Li, K. H. Chu and M. Toh, *Cancer Lett.*, 2010, **294**, 118–124; (*b*) J. K. Shen, H. P. Du, M. Yang, Y. G. Wang and J. Jin, *Ann. Hematol.*, 2009, **88**, 743–752.

23 E.-J. Lee, S.-Y. Oh and M.-K. Sung, *Food Chem. Toxicol.*, 2012, **50**, 4136–4143.

24 N. M. Weir, K. Selvendiran, V. K. Kutala, L. Tong, S. Vishwanath, M. Rajaram, S. Tridandapani, S. Anant and P. Kuppusamy, *Cancer Biol. Ther.*, 2007, **6**, 178–184.

25 G. Singh, A. Kaur, V. Sharma, N. Suri, P. R. Sharma, A. K. Saxena and M. P. S. Ishar, *MedChemComm*, 2013, **4**, 972–978.

26 S. Marchi, C. Giorgi, J. M. Suski, C. Agnoletto, A. Bononi, M. Bonora, E. DeMarchi, S. Missiroli, S. Patergnani, F. Poletti, A. Rimessi, J. Duszynski, M. R. Wieckowski and P. Pinton, *J. Signal Transduction*, 2011, **2012**, 1–17.

27 H. J. Kim, H.-J. Suh, J. H. Kim, S. Park, Y. C. Joo and J.-S. Kim, *J. Agric. Food Chem.*, 2010, **58**, 11633–11638.

28 D. Trachootham, J. Alexandre and P. Huang, *Nat. Rev. Drug Discovery*, 2009, **8**, 579–591.